

ORIGINAL ARTICLE

Mean Dose Constraint in Optimization Shells of a Lung SBRT Plan Helps further Reduce Normal Lung Dose

Tran Duc Hung ¹, Nguyen Thi Van Anh ², Le Manh Duc ², Quach Ngoc Mai ², Trinh Thi Mai ², Tran Kim Thoa ², Bui Quang Bieu ², Hoang Huu Thai ³, Pham Hong Lam ⁴, Nguyen The Thuong ⁵, Pham Quang Trung ^{1,2*} 

¹ School of Engineering Physics, Hanoi University of Science and Technology, Hanoi, Viet Nam

² Department of Radiation Oncology and Radiosurgery, 108 Military Central Hospital, Hanoi, Viet Nam

³ Department of Radiotherapy and Medical Physics - Nghe An Oncology Hospital, Nghe An, Viet Nam

⁴ 103 Military Hospital, Hanoi, Viet Nam

⁵ 175 Military Hospital, Ho Chi Minh, Viet Nam

*Corresponding Author: Pham Quang Trung

Received: 02 December 2024 / Accepted: 20 February 2025

Email: qtphamhus@gmail.com

Abstract

Purpose: This study aims to explore the effect of mean dose constraint in optimization shells on the reduction of normal lung dose in lung Stereotactic Body Radiation Therapy (SBRT) plans.

Materials and Methods: This study investigated 28 VMAT-based lung SBRT plans optimized with three artificial shells, which were re-generated with the same setup and an additional mean dose constraint besides the maximum dose limit. Dosimetric measurements of target volume and Organs At Risk (OARs) were compared between the original plans and re-generated ones using the Wilcoxon signed-rank test at 5% level significance (two-tailed).

Results: Replanning resulted in slight improvements in some parameters, such as R50% and the Gradient Measure (GM), which were reduced by 1.3% and 1.0%, respectively, with $p < 0.05$. However, there were slight increases in other parameters, such as D2cm and the maximum target dose, though these increases were not statistically significant. The Conformity Index (CI) remained nearly identical, with a mean value of 0.99 ± 0.03 for both original and re-optimized plans. Similarly, the V105% values were consistent, with mean values of $0.02 \pm 0.13\%$ in both groups. The parameters for dose deposited in normal lung tissue showed statistically significant reductions ranging from 1.0% to 1.7%. In addition, the mean dose to the spinal cord, esophagus, and skin was slightly reduced, but the mean dose to the heart showed a slight increase.

Conclusion: The study found that adding mean dose constraints to optimization shells in lung SBRT plans can reduce normal lung dose while maintaining dose conformity to the target. However, there may be slight changes in some OARs such as the spinal cord, esophagus, and skin. These changes were not statistically significant.

Keywords: Lung Stereotactic Body Radiation Therapy; Dose Falloff; Dose Gradient; Normal Lung Dose; Optimization Shells; Mean Dose Constraints.

1. Introduction

A good Stereotactic Body Radiation Therapy (SBRT) plan requires precise dose distribution that conforms to the target and rapidly drops off outside [1, 2]. SBRT can be delivered using Three-Dimensional Conformal Radiation Therapy (3D-CRT), Intensity-Modulated Radiation Therapy (IMRT), Volumetric-Modulated Arc Therapy (VMAT) and helical tomotherapy techniques [3-8]. VMAT and IMRT provide better target conformity than 3D-CRT, with VMAT offering comparable or slightly better quality than IMRT and reduced treatment time.

The inverse planning algorithms enable the implementation of various techniques to further optimize dose conformity while better-controlling dose gradients and hot spots outside the target area. One such technique is the Normal Tissue Objective (NTO) tool, which provides users of the Eclipse Treatment Planning System (TPS) with a straightforward approach to obtaining sharp dose gradients beyond the Planning Target Volume (PTV). The operation of this tool involves adjusting the configuration of an exponential decay dose-distance curve using four key parameters: start distance from the PTV border, start dose, end dose, and dose fall-off coefficient. Despite the ease of specifying NTO settings with minimal time and effort, determining the appropriate settings for a specific plan remains challenging [9]. Another method is to use optimization shells with well-defined dimensions and dose constraints. These shells are pseudo structures generated from the expansions of PTV Contour. Several groups have reported more conformal dose distributions of target volumes and lower radiation doses to normal organs when deploying 3 to 7 dose-limiting shells for VMAT- and IMRT-based plans in conventional fractionated radiotherapy and SBRT of different tumors, such as in spine, pancreas, cervical, prostate, lung [10-16]. Almost all of these studies assigned a single dose-limit constraint, which is usually the maximum dose, to each shell to facilitate quick dose fall-off outside the PTV [17, 18].

This study implemented an extra mean dose constraint to each optimization shell in VMAT-based SBRT plans for lung tumors, aiming to evaluate its effect on normal lung dose reduction and its potential to curb radiation pneumonitis – one of the most

common toxicities after lung SBRT. By addressing a novel aspect of lung SBRT treatment planning, the study incorporates mean dose constraints into optimization shells, a method that has received limited attention in the existing literature. While most research focuses on maximum dose constraints, this study explores how mean dose objectives can refine dose distribution and minimize radiation exposure to surrounding normal tissues. The clinical significance of this approach lies in its potential to reduce the risk of radiation pneumonitis, a prevalent and serious complication in lung SBRT. Demonstrating the feasibility and benefits of this methodology provides valuable insights that could enhance treatment efficacy and patient safety.

2. Materials and Methods

2.1. Patient Collection

28 clinically approved and implemented VMAT-based lung SBRT plans in 108 Military Central Hospitals were retrospectively reviewed and selected for this study.

All lung SBRT plans were performed based on four-Dimensional Computed Tomography (4DCT) data using Eclipse TPS version 13.6 (Varian Medical Systems, Palo Alto, California, USA). Treatment planning started with delineating targets and OARs using each phase of 4DCT and composite images derived from 4DCT scans, such as average intensity projection (AIP) and Maximum Intensity Projection (MIP). The Gross Tumor Volumes (GTV) were contoured on 10 phases of 4DCT, and combined to form a preliminary Internal Target Volume (ITV), which was then combined with ITV defined on the MIP image to obtain the final one. The finalized ITV was then transferred to the AIP image, where all dose computation was done. On the AIP image, we formed the PTV by adding a setup margin to the ITV, and contoured OARs such as the bilateral lungs, spinal cord, esophagus, heart, great vessels, and ribs according to RTOG 0813/0915 protocols [19, 20]. All structures were delineated, reviewed, and approved by experienced radiation oncologists before being used for planning. On our system, dose calculation was done using the Analytical Anisotropic Algorithm (AAA) and a grid size of 1.25 mm for SBRT plans.

Targets were prescribed with doses ranging from 30 to 60 Gy delivered in 1 to 10 fractions. To create SBRT treatment plans, the VMAT technique with one isocenter was used. All plans utilized three noncoplanar partial arcs, each configured with a specific collimator angle and a fixed couch rotation of either 0°, 10°, or 350°. The dose was delivered at a rate of 1400 MU/min using Flattening Filter-Free (FFF) photon beams at an energy of 6 MV. Beams were customized to avoid entrance through the contralateral lung, although exiting through it was unavoidable. All cases were delivered on TrueBeam™ STx (Varian Medical Systems, Palo Alto, California, USA), which was equipped with a high-definition 120 Multi Leaf Collimator (MLC).

2.2. Treatment Planning Methodology

We use the VMAT technique with three arcs for treatment planning, with fixed couch angles set at 0°, 350°, and 10°, respectively. This non-coplanar approach is designed to optimize beam angles, enhance target dose conformity, and minimize the dose delivered to surrounding critical structures. By varying couch angles, we achieve better sparing of organs at risk such as the heart and spinal cord while reducing entrance doses to healthy lung tissue. These configurations are particularly advantageous for complex tumor geometries or challenging anatomical locations.

With the help of the inverse planning algorithm, all treatment plans were designed to ensure the requirements of dose coverage at the target and the dose constraints at the OARs within the recommended limits or more stringent limits, as per the guidelines of RTOG 0813/0915, depending on tumor size, tumor location, and the patient's health status. Specifically, 100% prescription dose (Rx) is normalized to cover at

least 95% of the PTV. CI follows the definition provided by the Radiation Therapy Oncology Group (ratio of prescription isodose volume to PTV) is ideally less than 1.2, especially for very small tumors. V105% (volume outside the PTV receiving at least 105% Rx) should not exceed 15% of the PTV. R50% (ratio of 50% prescription isodose volume to PTV) should be within 2.9 to 5.9 depending on PTV sizes. D2cm (maximum dose at 2 cm from PTV in any direction) should range from 50% to 77% Rx according to different PTV sizes [19, 20].

To maximize the target dose, the PTV was split into PTV_{Opt1} (ITV) and PTV_{Opt2} (PTV excluding ITV).

Table 1 summarizes their dose constraints and priorities. PTV_{Opt1} aimed for a gradual dose fall-off from center to edge, with three limit levels of the Dose-Volume Histogram (DVH) ensuring a larger ITV portion received higher doses. PTV_{Opt2} targeted faster dose fall-off using a single limit. Lower doses within PTV were prioritized (100 or 120) to maximize the dose. Maximum dose in PTV_{Opt2} was constrained to prevent exceeding 105% Rx. Priority for 130% Rx max dose in PTV_{Opt1} was lower due to acceptable dose inhomogeneity, with typical 160% Rx max point doses in PTV.

To control dose spillage, three optimization shells surrounded the PTV, enhancing conformity and gradient. Shells, not overlapping, were defined between concentric rings around PTV, cut if extending beyond the body. Rings were created by expanding 1, 10, 20, and 50 mm from the PTV border to uniformly control dose falloff in all directions. Each shell (1 through 3, Figure 1) was assigned a maximum dose constraint

Table 1. Dose constraints for target volume and optimization shells in original plans

	Volume (%)	Lower Dose Limit (% of Rx)	Upper Dose Limit (% of Rx)	Priority (relative number)
PTV _{Opt1} = ITV	0	-	130	30
	33.33	120	-	120
	66.66	112	-	120
	100	105	-	100
PTV _{Opt2} = PTV - ITV	0	-	104	120
	100	100	-	100
Shell 1	0	-	60	60
Shell 2	0	-	40	60
Shell 3	0	-	30	60

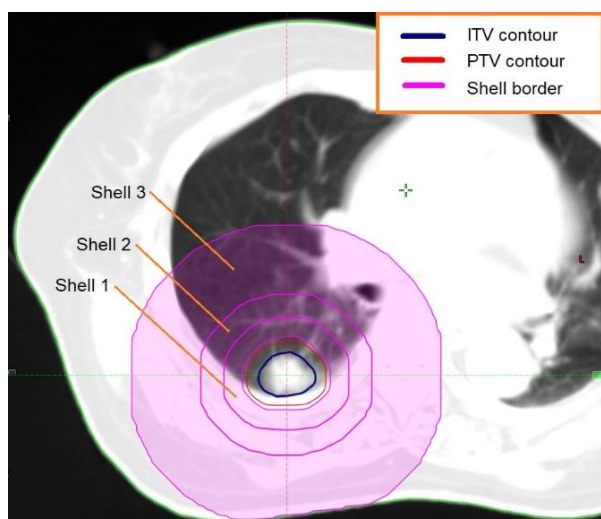


Figure 1. A cross-sectional view showing ITV, PTV, and three optimization shell

As show in Table 2, each row corresponds to a treatment planning shell, detailing its position relative to the PTV, its specific purpose, and the applied dose constraint.

Dose constraints specified for optimization shells are shown in Table 3. With the purpose of minimizing the maximum doses to OAR and non-critical organs, which were not contoured as OAR and possibly less susceptible to the radiation, only constraints on the maximum dose were set for each shell. To push the optimization towards the desired outcome, the dose constraints were set to be slightly more stringent than the standard values. Priorities were determined through empirical observations and may require modification, for example 10% deviation, in certain cases. The thickness of shells was also partly based on our experiences and investigation of the relationship between dose drop speed at specific distances. The

thinnest shell (9 mm) was thicker than the calculation grid of 1.25 mm, thus we had a continuous structure regardless of data fluctuations.

Table 3. Dose constraints for optimization shells in

	Volume (%)	Mean Dose Limit (% of Rx)	Upper Dose Limit (% of Rx)	Priority (relative number)
Shell 1	0	-	60	60
	-	43	-	60
Shell 2	0	-	40	60
	-	32	-	60
Shell 3	0	-	30	60
	-	-	-	-

In our treatment planning approach, OAR constraints are applied based on the proximity of the organ to the PTV. If an OAR is located far from the PTV, constraints are not necessary, as the dose to that structure is inherently low. However, when an OAR is near the PTV, we introduce dose constraints with a priority of approximately 50 to ensure dose limitation without overly compromising target coverage. In cases where the OAR overlaps with the PTV, we assign a higher priority of around 100 to strictly enforce dose constraints while balancing the need for adequate tumor coverage (Table 4).

Additionally, manual NTO was employed across all treatment plans. For lung SBRT plans at our institution, the manual NTO parameters were set as follows: Priority (100), Distance from target border (0.1 cm), Start dose (105% of prescription dose), End dose (60% of prescription dose), and Fall-off (0.5).

Table 2. Description and Dose Constraints for Optimization Shells in SBRT Planning

Shell	Description	Maximum Dose Constraint	Influence on Parameters
Shell 1	Controls high dose spillage near PTV, promoting dose conformity. 1 mm gap between shell and PTV allows prescription isodose to fall within. Maximum dose set at 60% Rx.	60% Rx	CI, V105%, R50%, D2cm
Shell 2	Controls intermediate dose spillage. Facilitates steep dose gradient limiting 50% isodose curve within 1-2 cm from PTV. Maximum dose below 50% Rx.	Below 50% Rx	R50%, D2cm
Shell 3	Minimizes low dose distributions and residual hot spots distant from PTV. Inner border 2 cm from PTV enforces D2cm criterion (50%-77% Rx). Maximum dose around 30% Rx.	Around 30% Rx	D2cm

Table 4. Organ-at-Risk (OAR) Dose Constraints and Priorities for Lung SBRT Based on Fractionation Schemes

OAR	1 Fraction (Gy)	3 Fractions (Gy)	5 Fractions (Gy)	10 Fractions (Gy)	Priority (0–100)
Spinal Cord	≤ 14.0	≤ 18.0	≤ 30.0	≤ 45.0	50–100
Esophagus	≤ 15.4 V10 < 5 cc	≤ 27.0 V18.9 < 5 cc	≤ 30.0 V22.5 < 5 cc	≤ 50.0 , V30 < 5 cc	50–100
Trachea/Bronchus	≤ 20.2	≤ 30.0	≤ 40.0	≤ 50.0	50–100
Heart/Pericardium	≤ 22.0 V10 < 15 cc	≤ 30.0 V15 < 15 cc	≤ 38.0 V22.5 < 15 cc	≤ 45.0 V30 < 15 cc	50–100
Great Vessels	≤ 37.0 , V20 < 10 cc	≤ 45.0 V39 < 10 cc	≤ 53.0 V45 < 10 cc	≤ 60.0 V50 < 10 cc	50–100
Chest Wall	V20 < 30 cc	V30 < 30 cc	V30 < 30 cc	V40 < 30 cc	50–100
Brachial Plexus	≤ 17.5	≤ 24.0	≤ 27.2	≤ 40.0	50–100
Healthy Lung	V20 < 10%,	V20 < 10%,	V20 < 10%	V20 < 10%	50–100
(Total Lung - PTV)	V12.5 < 15%	V12.5 < 15%	V12.5 < 15%	V12.5 < 15%	50–100
Stomach	≤ 12.4	≤ 20.0	≤ 27.2	≤ 40.0	50–100
OARs far from PTV	No constraint applied	No constraint applied	No constraint applied	No constraint applied	0

2.3. Treatment Replanning Methodology

Using the original plans as the starting point, we examined the effect of adding another dose constraint to optimization structures in terms of dose spreading to normal lungs, which contributes to radiation pneumonitis. All 28 VMAT-based lung SBRT plans were re-generated with the same setup except that each optimization shell received an additional mean dose constraint besides the maximum dose limit. Parameters of shells are summarized in Table 3.

Mean dose constraints were selected to be less than 20% of the dose range between the inner and outer borders of corresponding shells to force a steep dose gradient within these shells, thus pushing high doses towards the PTV. With the same dose range between the two borders, a lower mean dose constraint was

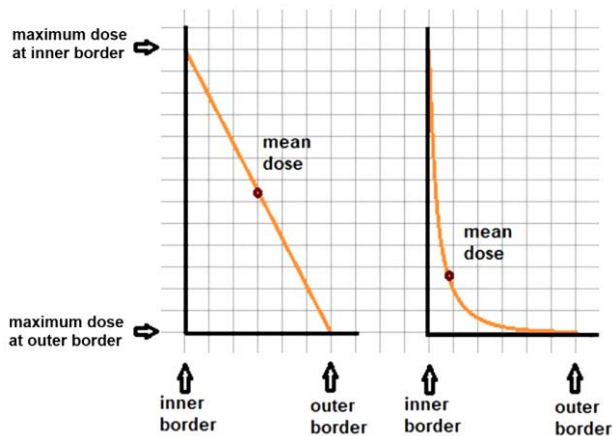


Figure 2. Theoretical illustration of dose fall off with different mean dose constraints indicated by dark red dots

expected to enforce a steeper dose gradient line (Figure 2).

2.4. Evaluation of Plan Quality

The evaluation criteria for the target and dose spillage, as well as the parameters for OARs to assess the plan, are presented in Table 5 [19, 20].

2.5. Statistical Analysis

All parameters for target volume, dose spillage, and OARs discussed in the section on Evaluation of plan quality were included in the statistical analysis. Dosimetric measurements of both original plans and re-generated ones, including CI, R50%, D2cm, V105%, and V20, were plotted as a function of PTV size and compared with dosimetric acceptability per RTOG 0813/0915 protocols.

Wilcoxon signed-rank test was used to compare differences between the two treatment plans. The statistical significance was assessed using a two-sided p-value < 0.05.

3. Results

3.1. Details of the Enrolled Cases

A total of 28 VMAT-based lung SBRT plans were enrolled in this study. The PTV volumes of the

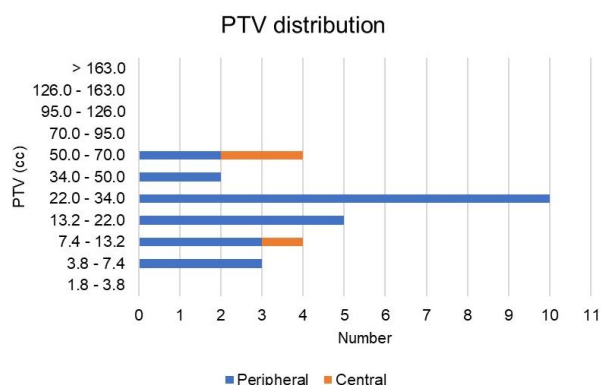


Figure 3. Distribution of the size of 28 PTVs selected in this study

selected plans varied between 4.1 to 65.1 cc (mean \pm standard deviation = 26.5 ± 16.5 cc), including 25(89.3%) peripheral and 3 (10.7%) central tumors. Tumors located within a 2-cm radius of the airway or mediastinal pleura were considered central, while those outside this range were considered peripheral. The frequency distribution of PTV volumes is shown in Figure 3, with volume bins based on the guidelines of RTOG 0813/0915 [19, 20].

3.2. Evaluation of parameters for PTV and dose spillage

The CI values for both original and regenerated plans were almost identical and well below the minimum threshold of 1.2 specified in RTOG 0813/0915 protocols [19, 20]. The V105% values remained consistent after replanning, with 27 out of 28 cases having values near 0%, and the remaining case recording a value of 0.68%, which is well below the acceptable tolerance of 15% specified in the protocols.

Replanning resulted in improvements of 1.3% in R50% (from 4.00 ± 0.62 to 3.95 ± 0.64) and 1.0% in

GM (from 1.01 ± 0.16 to 1.00 ± 0.17), both statistically significant ($p < 0.05$). There was an increase in D2cm from $50.83 \pm 3.99\%$ to $51.14 \pm 4.23\%$ and in Maximum Target Dose from $146.47 \pm 7.07\%$ to $147.15 \pm 6.24\%$, though neither change was statistically significant ($p > 0.2$). Table 6 presents a comparison of the dosimetric parameters for all plans. The CI, R50%, and D2cm (%) for both the original and revised plans were evaluated against PTV (cc) and compared with the lower and upper bounds specified in the RTOG 0813/0915 protocols [19, 20]. The CI values were very close to the ideal value of 1, while the R50% and D2cm values were very close to the lower bounds. Figure 4, Figure 5, and Figure 6 plot CI, R50%, and D2cm (%) for the original and revised plans against PTV (cc), along with the lower and upper bounds specified in RTOG 0813/0915 protocols.

Figure 7 shows an example of two plans of the same tumor, which visually exhibited little differences in dose distribution. The left one is an original plan, and the corresponding replan is depicted on the right. The 3D orthogonal views show the contours of the PTV (in red) enclosed by the 50% prescription isodose contour (in orange), which becomes smaller after replanning. The values of R50% (3.57) and GM (1.02 cm) in the original plan were decreased to 2.93 and 1.00 cm, respectively.

3.3. Evaluation of Parameters for OARs

All of the plans met the RTOG 0813/0915 protocols for the doses to normal lung, spinal cord, esophagus, heart, skin, and other OARs. Table summarizes the changes in parameters for both groups of plans. With the effect of mean dose constraints in replanning methodology, the dose deposited into normal lung

Table 5. Plan evaluation criteria and parameters for OARs

Metric	Details
Target and Dose Spillage	CI, GM (cm), R50%, D2cm (%Rx), V105% (%PTV), Max target dose (%Rx)
Parameters for OARs	Normal lung V20 (%), Normal lung V10 (%), Mean lung dose MLD (cGy), Mean dose of Spinal Cord (cGy), Mean dose of Heart (cGy), Mean dose of Esophagus (cGy), Mean dose of Skin (cGy)
Monitor units (MUs)	The number of MUs was also a parameter to be monitored in a treatment plan.
Patient-Specific Quality Assurance	Gamma pass rate of greater than 95% using 2%/1mm criteria. This ensures the treatment plan's accuracy and safety

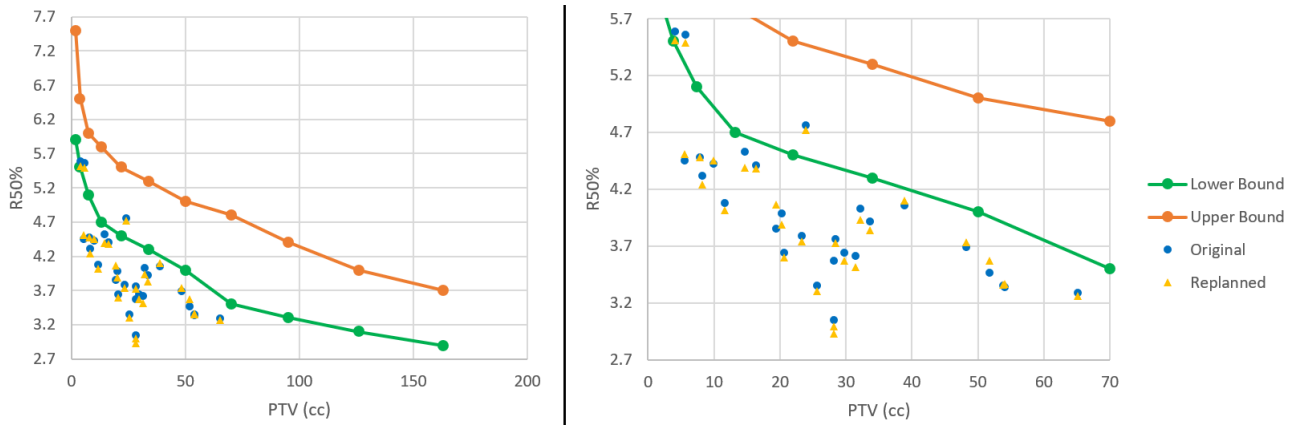


Figure 5. Plot of R50% against PTV of all plans together with lower and upper bounds of RTOG 0813/0915. Range of investigated plans are scaled on the right

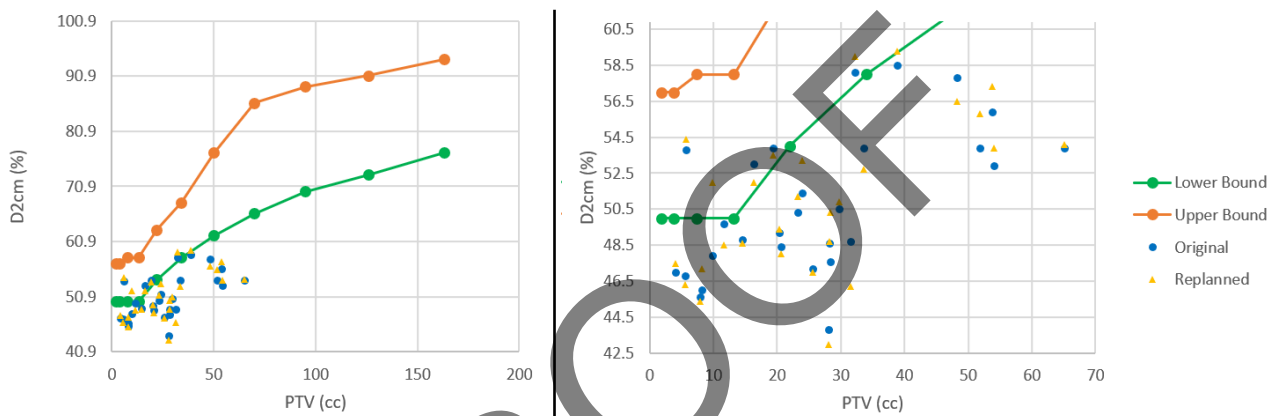


Figure 6. Plot of D2cm against PTV of all plans together with lower and upper bounds of RTOG 0813/0915. Range of investigated plans are scaled on the right

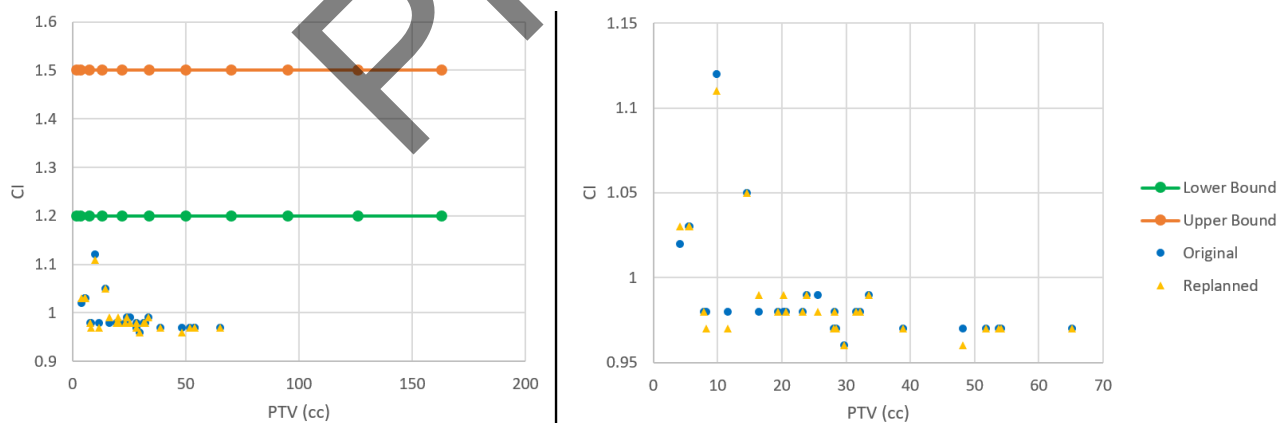


Figure 4. Plot of CI against PTV of all plans together with lower and upper bounds of RTOG 0813/0915. Range of investigated plans are scaled on the right

tissue was found to be significantly reduced ($p < 0.05$). The mean values of V20, V10, and MLD were lowered from 3.47% to 3.41% (a reduction of 1.7%), 7.73% to 7.60% (a reduction of 1.7%), and 301.66cGy to 298.51cGy (a reduction of 1.0%), respectively. The

V20 values for both the original and revised plans, evaluated against PTV (cc), were notably below the lower bounds specified in the RTOG 0813/0915 protocols [19, 20].

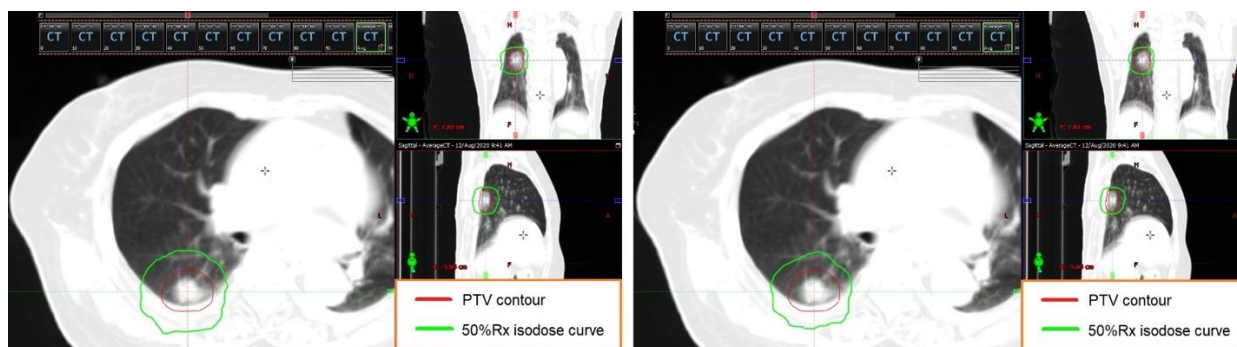


Figure 7. Orthogonal views of a representative tumor on original (right) and revised (left) plan showing the PTV, and 50% prescription isodose curve

Table 6. Comparison of target and dose spillage parameters for all original and re-optimized plans

Metric	Original	Replanned	p-value
CI	0.99 ± 0.03	0.99 ± 0.03	> 0.2
R50%	4.00 ± 0.62	3.95 ± 0.64	< 0.05
D2cm (%)	50.83 ± 3.99	51.14 ± 4.23	> 0.2
GM (cm)	1.01 ± 0.16	1.00 ± 0.17	< 0.05
Max target dose (%)	146.47 ± 7.07	147.15 ± 6.24	> 0.2
V105% (%)	0.02 ± 0.13	0.02 ± 0.13	> 0.2

The mean dose to the spinal cord, esophagus, and skin were reduced in the revised plans as compared to the original ones. However, the differences did not reach statistical significance ($p > 0.2$). The mean dose to the heart in the re-generated plans showed a slight increase, but the change was not statistically significant ($p > 0.2$).

3.4. Evaluation of Other Parameters

Replanning led to an increase in the mean number of MUs, from 3789.39 to 3856.08 (Table 7). However, this change was not statistically significant ($p > 0.2$). This increase can be attributed to the additional optimization requirements introduced by the mean dose constraints in the optimization shells, which necessitated higher beam modulation and fluence to achieve the desired dose distributions and ensure steeper dose gradients around the PTV.

Patient-specific quality assurance: All plans achieved a gamma pass rate greater than 95% for all fields using the critical 2%/1mm criteria.

4. Discussion

In this retrospective study, we present our experience with lung Stereotactic Body Radiotherapy (SBRT) using a dose optimization technique for target volumes and organs at risk (OARs). We further explored the potential for reducing normal lung tissue toxicity by implementing mean dose constraints in artificial shells around the Planning Target Volume

Table 7. Comparison of dose to OARs and MU for all original and re-optimized plans

Metric	Original	Replanned	p-value
Normal lung V10 (%)	7.73 ± 4.34	7.60 ± 4.25	< 0.05
Normal lung V20 (%)	3.47 ± 1.95	3.41 ± 1.91	< 0.05
Normal lung MLD (cGy)	301.66 ± 136.53	298.51 ± 134.55	< 0.05
Spinal Cord D_{av} (cGy)	139.73 ± 94.53	137.00 ± 90.54	> 0.2
Heart D_{av} (cGy)	169.79 ± 148.74	171.70 ± 151.77	> 0.2
Esophagus D_{av} (cGy)	234.30 ± 149.44	231.52 ± 151.99	> 0.2
Skin D_{av} (cGy)	55.91 ± 26.24	55.20 ± 26.15	> 0.2
MU	3789.39 ± 1918.01	3856.08 ± 1897.45	> 0.2

(PTV). Our results indicate that all plans, both original and revised, met the dosimetric standards for target Conformity (CI) and OARs outlined in the RTOG 0813/0195 protocols, although none of the revised plans were used for actual patient treatment. This aligns with the findings of previous studies, which have shown that dose optimization can meet clinical dosimetric criteria for target volumes and OARs in lung SBRT [1, 2].

Following replanning, we observed a reduction in the dose metrics R50% and GM by 1.3% and 1.0%, respectively, with $p < 0.05$, while CI and V105% remained unchanged. These findings are consistent with prior studies that suggest modest improvements in dose falloff near the PTV, particularly with adjustments to dose constraints for surrounding tissues [21]. However, unlike previous studies that linked dose falloff with distance from the PTV, our study specifically examined the potential clinical relevance of metrics such as R50% and D2cm to concerning toxicity scores, an area where clinical data is currently lacking. This highlights a gap in the literature that our study begins to address.

For OARs, our findings indicate that mean dose constraints resulted in statistically significant reductions ($p < 0.05$) in dose to normal lung tissue, including V10, V20, and MLD. These parameters are well-documented as being associated with radiation pneumonitis [22-26], and similar associations with overall survival have been reported in stage I lung cancer [24]. These results support the conclusions of previous studies, such as those by Duan *et al.* [13], who demonstrated that the reduction of dose to normal lung tissue is achievable through optimization techniques, though their study did not focus on the specific metrics used here. Our work adds to this by emphasizing the role of dose constraints in reducing lung toxicity without adversely affecting other OARs, as evidenced by the lack of statistically significant differences in dose to the spinal cord, heart, esophagus, and skin.

While we adopted the dose tolerances outlined in the RTOG 0813/0915 protocols as a baseline for optimization, it is important to note that these should be viewed as a starting point for further refinement. The dose limits configured for optimization shells in our study were based on empirical observations from our center. This is in contrast to several other studies,

such as those by Desai *et al.* [12], which focused on a fixed number of shells with predefined constraints. Our approach, using a more flexible set of optimization shells, acknowledges the variation in PTV sizes and the dose gradients observed in clinical practice. This contrasts with other studies that have employed either fewer shells or fixed shell designs. For example, Duan *et al.* [13] examined the impact of 2 to 8 optimization shells, concluding that the addition of more than six shells did not significantly improve plan quality, but did increase optimization time. Our findings support this conclusion, as we found only marginal improvements in dose distribution with additional shells. However, we also recognize that the optimal shell configuration may vary with larger PTV volumes. Our study cohort, consisting of small to medium PTVs (4.1 to 65.1 cc), may not represent the full range of clinical cases. Larger PTV volumes (>70.0 cc) may require a more customized approach, incorporating modified shell thicknesses or dose constraints that vary based on PTV volume, as suggested in previous studies [11, 21, 27, 28].

The Anisotropic Analytical Algorithm (AAA) in Eclipse is widely used for dose calculations due to its efficiency and ability to model photon interactions in homogeneous tissues. However, in heterogeneous regions like the lungs, AAA can experience dosimetric inaccuracies, such as overestimating the dose in low-density tissues due to limited modeling of photon scattering at tissue interfaces. While AAA is generally accurate for many treatment sites, its performance may be less reliable in areas with significant tissue variation. Clinicians should be mindful of these limitations, especially when planning treatments for lung cancer, and consider supplementary verification methods or alternative algorithms for critical dose points. In summary, while AAA in Eclipse is a reliable and efficient tool for dose calculation, its limitations in heterogeneous regions, such as the lung, must be considered in treatment planning. Further research and development of more accurate algorithms, such as Monte Carlo-based techniques, may provide improvements in dose accuracy in such challenging regions.

While the number of Monitor Units (MUs) increased slightly by 1.8% after replanning, this change was not statistically significant. This is in line with the results of other studies, such as those by

Huang *et al.* [29], who observed negligible changes in MUs following dose optimization. One limitation of our study, not considered in previous work, is the impact of processing time during plan optimization. In our center, the optimization process of the Treatment Planning System (TPS) is influenced by the concurrent load on the system, which may affect processing time. This aspect should be further explored in future studies to better understand the trade-off between plan quality and optimization time.

5. Conclusion

Besides maximum dose constraints, adding mean dose constraints to optimization shells can reduce normal lung dose while maintaining dose conformity to the target. However, there may be a slight increase in D2cm and a minor decrease in OARs such as the spinal cord, esophagus, and skin, although these changes were not statistically significant.

References

- 1- David Hoffman, Irena Dragojević, Jeremy Hoisak, David Hoopes, and Ryan Manger, "Lung Stereotactic Body Radiation Therapy (SBRT) dose gradient and PTV volume: a retrospective multi-center analysis." (in eng), *Radiation oncology (London, England)*, Vol. 14 (No. 1), pp. 162-62, (2019).
- 2- M. Uematsu *et al.*, "Computed tomography-guided frameless stereotactic radiotherapy for stage I non-small cell lung cancer: a 5-year experience." (in eng), *International journal of radiation oncology, biology, physics*, Vol. 51 (No. 3), pp. 666-70, (2001).
- 3- Marta Adamczyk, Marta Kruszyna-Mochalska, Anna Rucińska, and Tomasz Piotrowski, "Software simulation of tumour motion dose effects during flattened and unflattened ITV-based VMAT lung SBRT." *Reports of Practical Oncology & Radiotherapy*, Vol. 25 (No. 4), pp. 684-91, (2020).
- 4- Serena Badellino *et al.*, "No differences in radiological changes after 3D conformal vs VMAT-based stereotactic radiotherapy for early stage non-small cell lung cancer." (in eng), *The British journal of radiology*, Vol. 90 (No. 1078), pp. 20170143-43, (2017).
- 5- C. Herbert *et al.*, "Stereotactic body radiotherapy: volumetric modulated arc therapy versus 3D non-coplanar conformal radiotherapy for the treatment of early stage lung cancer." (in eng), *Technology in Cancer Research & Treatment*, Vol. 12 (No. 6), pp. 511-16, (2013).
- 6- Andrea Holt, Corine van Vliet-Vroegindeweij, Anton Mans, José S. Belderbos, and Eugène M. F. Damen, "Volumetric-modulated arc therapy for stereotactic body radiotherapy of lung tumors: a comparison with intensity-modulated radiotherapy techniques." (in eng), *International journal of radiation oncology, biology, physics*, Vol. 81 (No. 5), pp. 1560-67, (2011).
- 7- Chin Loon Ong, Wilko F. A. R. Verbakel, Johan P. Cuijpers, Ben J. Slotman, Frank J. Lagerwaard, and Suresh Senan, "Stereotactic radiotherapy for peripheral lung tumors: a comparison of volumetric modulated arc therapy with 3 other delivery techniques." (in eng), *Radiotherapy and oncology : journal of the European Society for Therapeutic Radiology and Oncology*, Vol. 97 (No. 3), pp. 437-42, (2010).
- 8- Masahide Saito *et al.*, "Evaluation of the target dose coverage of stereotactic body radiotherapy for lung cancer using helical tomotherapy: A dynamic phantom study." *Reports of Practical Oncology & Radiotherapy*, Vol. 25 (No. 2), pp. 200-05, (2020).
- 9- Liza I. Ndrayani, Choirul A. Nam, Heri S. Utanto, and Rinarto S. Ubrot, "Normal tissue objective (NTO) tool in Eclipse treatment planning system for dose distribution optimization." *Polish Journal of Medical Physics And Engineering*, Vol. 28 (No. June), pp. 99-106, (2022).
- 10- Daniel Buerge *et al.*, "Fully automated treatment planning of spinal metastases - A comparison to manual planning of Volumetric Modulated Arc Therapy for conventionally fractionated irradiation." (in eng), *Radiation oncology (London, England)*, Vol. 12 (No. 1), pp. 33-33, (2017).
- 11- Yangsen Cao *et al.*, "Optimization of dose distributions of target volumes and organs at risk during stereotactic body radiation therapy for pancreatic cancer with dose-limiting auto-shells." (in eng), *Radiation oncology (London, England)*, Vol. 13 (No. 1), pp. 11-11, (2018).
- 12- Dharmin Desai *et al.*, "Cleaning the dose falloff in lung SBRT plan." (in eng), *Journal of applied clinical medical physics*, Vol. 22 (No. 1), pp. 100-08, (2021).
- 13- Yanhua Duan *et al.*, "On the optimal number of dose-limiting shells in the SBRT auto-planning design for peripheral lung cancer." (in eng), *Journal of applied clinical medical physics*, Vol. 21 (No. 9), pp. 134-42, (2020).
- 14- Abdul Wahab M. Sharfo, Peter W. J. Voet, Sebastiaan Breedveld, Jan Willem M. Mens, Mischa S. Hoogeman, and Ben J. M. Heijmen, "Comparison of VMAT and IMRT strategies for cervical cancer patients using automated planning." (in eng), *Radiotherapy and oncology : journal of the European Society for Therapeutic Radiology and Oncology*, Vol. 114 (No. 3), pp. 395-401, (2015).
- 15- Osamu Tanaka *et al.*, "Stereotactic body radiation therapy to the spine: contouring the cauda equina instead of the spinal cord is more practical as the organ at risk."

- Reports of Practical Oncology and Radiotherapy*, Vol. 28 (No. 3), pp. 407-15, (2023).
- 16- Peter W. J. Voet, Maarten L. P. Dirksen, Sebastiaan Breedveld, and Ben J. M. Heijmen, "Automated generation of IMRT treatment plans for prostate cancer patients with metal hip prostheses: comparison of different planning strategies." (in eng), *Medical physics*, Vol. 40 (No. 7), pp. 71704-04, (2013).
 - 17- Kirk Luca *et al.*, "A lung SBRT treatment planning technique to focus high dose on gross disease." *Medical Dosimetry*, 2024/09/10/ (2024).
 - 18- X. Qian *et al.*, "The optimal stereotactic body radiotherapy dose with immunotherapy for pulmonary oligometastases: a retrospective cohort study." (in eng), *J Thorac Dis*, Vol. 16 (No. 10), pp. 7072-85, Oct 31 (2024).
 - 19- Andrea Bezjak *et al.*, "Safety and Efficacy of a Five-Fraction Stereotactic Body Radiotherapy Schedule for Centrally Located Non-Small-Cell Lung Cancer: NRG Oncology/RTOG 0813 Trial." (in eng), *Journal of clinical oncology : official journal of the American Society of Clinical Oncology*, Vol. 37 (No. 15), pp. 1316-25, (2019).
 - 20- Gregory M. M. Videtic *et al.*, "A Randomized Phase 2 Study Comparing 2 Stereotactic Body Radiation Therapy Schedules for Medically Inoperable Patients With Stage I Peripheral Non-Small Cell Lung Cancer: NRG Oncology RTOG 0915 (NCCTG N0927)." (in eng), *International journal of radiation oncology, biology, physics*, Vol. 93 (No. 4), pp. 757-64, (2015).
 - 21- Ganesh Narayanasamy, Dharmin Desai, Sanjay Maraboyina, Jose Penagaricano, Robert Zwicker, and Ellis Lee Johnson, "A Dose Falloff Gradient Study in RapidArc Planning of Lung Stereotactic Body Radiation Therapy." (in eng), *Journal of medical physics*, Vol. 43 (No. 3), pp. 147-54, (2018).
 - 22- Houda Bahig *et al.*, "Excellent Cancer Outcomes Following Patient-adapted Robotic Lung SBRT But a Case for Caution in Idiopathic Pulmonary Fibrosis." (in eng), *Technology in Cancer Research & Treatment*, Vol. 14 (No. 6), pp. 667-76, (2015).
 - 23- Ryan Baker *et al.*, "Clinical and dosimetric predictors of radiation pneumonitis in a large series of patients treated with stereotactic body radiation therapy to the lung." (in eng), *International journal of radiation oncology, biology, physics*, Vol. 85 (No. 1), pp. 190-95, (2013).
 - 24- Guillaume Dupic *et al.*, "Significant Correlation Between Overall Survival and Mean Lung Dose in Lung Stereotactic Body Radiation Therapy (SBRT)." (in eng), *Frontiers in oncology*, Vol. 10pp. 1577-77, (2020).
 - 25- Eileen M. Harder, Henry S. Park, Zhe Chen, and Roy H. Decker, "Pulmonary dose-volume predictors of radiation pneumonitis following stereotactic body radiation therapy." *Practical Radiation Oncology*, Vol. 6 (No. 6), pp. e353-e59, (2016).
 - 26- Jing Zhao *et al.*, "Simple Factors Associated With Radiation-Induced Lung Toxicity After Stereotactic Body Radiation Therapy of the Thorax: A Pooled Analysis of 88 Studies." (in eng), *International journal of radiation oncology, biology, physics*, Vol. 95 (No. 5), pp. 1357-66, (2016).
 - 27- Dharmin D. Desai, Ivan L. Cordrey, and E. L. Johnson, "A physically meaningful relationship between R50% and PTV surface area in lung SBRT." (in eng), *Journal of applied clinical medical physics*, Vol. 21 (No. 9), pp. 47-56, (2020).
 - 28- Dharmin D. Desai, E. L. Johnson, and Ivan L. Cordrey, "An analytical expression for R50% dependent on PTV surface area and volume: a lung SBRT comparison." (in eng), *Journal of applied clinical medical physics*, Vol. 21 (No. 11), pp. 278-82, (2020).
 - 29- B. T. Huang, Z. Lin, P. X. Lin, J. Y. Lu, and C. Z. Chen, "Monitor unit optimization in stereotactic body radiotherapy for small peripheral non-small cell lung cancer patients." (in eng), *Sci Rep*, Vol. 5p. 18453, Dec 18 (2015).